

Observation of Spin Precession in GaAs Inversion Layers Using Antilocalization

P. D. Dresselhaus, C. M. A. Papavassiliou,^(a) and R. G. Wheeler

Department of Applied Physics, Yale University, New Haven, Connecticut 06520-2157

R. N. Sacks

United Technologies Research Center, East Hartford, Connecticut 06108

(Received 8 July 1991)

Nearly-zero-field magnetoconductance measurements have been used to deduce the conduction-band spin splitting of GaAs. The dominant spin-scattering mechanism is the randomization of spin precession due to elastic scattering. By independently controlling electron density and mobility, it is observed that the crystal-field-induced spin splitting is the cause of the spin-orbit scattering. This technique is used to infer the band-structure splitting parameter, $a_{42} = 26.1 \pm 0.9 \text{ eV \AA}^3$.

PACS numbers: 71.25.Tn, 71.70.Ej, 72.20.Fr, 73.20.Fz

The spin-split character of the conduction band in zinc-blende structures [1] has not been observed in a zero-magnetic-field transport measurement. Analogous to spin-orbit splitting, an electric field transformed into the reference frame of a moving electron acts as a magnetic field which removes the spin degeneracy. These electric fields arise from the polar nature of III-V materials augmented by an inversion field in a heterostructure. There have been several experiments which have investigated these zero-field spin splittings. From an analysis of the beat patterns observed in Shubnikov-de Haas oscillations, the zero-field splitting has been deduced from high-magnetic-field measurements in InGaAs/InAlAs [2] and GaSb-InAs [3]. A linear extrapolation of electron-spin-resonance energies to zero magnetic field has been used in GaAs-AlGaAs heterostructures to deduce a lower bound to the zero-field spin splitting of $32 \mu\text{eV}$ for a density of $N_s = 4.6 \times 10^{15} \text{ m}^{-2}$ [4]. Optical spin orientation has been used in bulk $\text{Al}_x\text{Ga}_{1-x}\text{As}$ [5] and in GaAs [6] to measure spin-relaxation times at zero field, from which an estimate of the splitting was made. Here we report a determination of this splitting ΔE_c deduced from a quantum conductance measurement using GaAs heterostructures in a magnetic field of a few gauss.

The interference between time-reversed paths leads to the weak-localization contribution to the quantum conductance. Spin-coherent paths constructively interfere to cause a reduction in conductivity while the spin-dephased paths destructively interfere to cause an enhanced conductivity. Since a perpendicular magnetic field destroys the interference in both cases, one observes the antilocalization signature of a low-field magnetoresistance followed by a magnetoconductance. We have used measurements of this weak antilocalization as a probe of the spin-dephasing rate which we find to be related to the band structure. Kawaji *et al.* [7] were the first to observe antilocalization in this system. They measured a spin-orbit scattering rate in devices similar to ours, but could not quantitatively explain the effect. In contrast to spin-orbit scattering in metal films [8], we find that the spin-relaxation mechanism is not due to scattering by heavy impurities, but is caused by the underlying band struc-

ture. The lack of mobility dependence will be used to show that the actual spin-dephasing mechanism is that described by D'yakanov and Perel' (DP) [9]. The density dependence will be used to show that the spin-orbit scattering in GaAs heterostructures is primarily determined by the crystal field, not the inversion field.

In a weak-localization experiment one measures the quantum correction to the conductance which has the form [10]

$$\Delta\sigma = \frac{-e^2}{2\pi^2\hbar} \left\{ \Psi \left(\frac{1}{2} + \frac{H_{tr}}{B} \right) - \Psi \left(\frac{1}{2} + \frac{H_2}{B} \right) + \frac{1}{2} \left[\Psi \left(\frac{1}{2} + \frac{H_\phi}{B} \right) - \Psi \left(\frac{1}{2} + \frac{H_4}{B} \right) \right] \right\}, \quad (1)$$

where B is the applied magnetic field, Ψ is the digamma function, $H_2 = H_\phi + 2H_{s.o.}^x + 2H_{s.o.}^z$, $H_4 = H_\phi + 4H_{s.o.}^x$, and $H_a = \hbar/4De\tau_a$, D being the diffusivity, given by $\frac{1}{2}v_f^2\tau_{tr}$, and the a 's correspond to tr =transport, $s.o.$ =spin orbit, or ϕ =phase breaking. We use magnetic-field scales H_a because they are the physically measured quantities, and are interpreted as of the order of the maximum field at which the relevant scattering rate affects the quantum interference. Equation (1) assumes that all interfering path lengths are much longer than the mean free path. We interpret this as limiting its validity to magnetic fields $\lesssim 0.5H_{tr}$. Figure 1 shows a typical magnetoconductance trace along with a fit by Eq. (1). The dipped structure in the conductance is characteristic of the presence of spin-orbit scattering ($H_{s.o.} > H_\phi$). Simulations show that the minimum conductance occurs at a field of $\sim 4H_{s.o.}$ if $H_{s.o.} \gg H_\phi$.

We consider two possible spin-dephasing processes that could give rise to this spin-orbit scattering: the spin-orbit coupling associated with the electric field of an impurity (the Elliott mechanism), or the randomization of the spin by elastic scattering in a material with a spin-split energy level (the DP mechanism). The Elliott mechanism [11] is most effective if the scattering is by heavy impurities located in the inversion layer. The spin-orbit rate is pre-

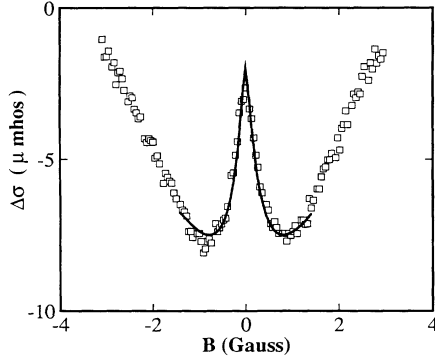


FIG. 1. Magnetoconductance trace, $\Delta\sigma(B) - \Delta\sigma(4 \text{ G})$, for 1017-C2a with $N_s = 5.1 \times 10^{15} \text{ m}^{-2}$ and $H_{tr} = 2.81 \text{ G}$ at $T = 1.0 \text{ K}$. The solid curve is a fit by Eq. (1) with $H_{s.o.} = 0.187 \text{ G}$ and $H_p = 0.028 \text{ G}$. The fit is valid for $B < 1.4 \text{ G}$. Note that the minimum occurs at $B \sim 4H_{s.o.}$.

dicted to be

$$\tau_{s.o.}^{-1} = 2\pi(g-2)^2 R^2 N_s \tau_{tr}^{-1}, \quad (2)$$

where g is the conduction-band g factor and R is of the order of the atomic radius of the scatterer. This theory predicts a linear relationship between the spin-orbit scattering rate and the transport scattering rate, $H_{s.o.} \propto H_{tr}$. The DP mechanism applies provided that the impurity broadening is much larger than the spin splitting ($\hbar \tau_{tr}^{-1} > \Delta E_c$, i.e., the electron scatters before it reaches an eigenstate of the system). For a two-dimensional electron gas, the spin splitting will act as an effective magnetic field in the plane, directed perpendicular to the motion with a $\sin(2\theta)$ angular factor relative to the (100) axis. Thus, the electronic spin will precess about an axis perpendicular to its motion [5,9,12]. For this case, we use the relationship $H_{s.o.} = 2H_{s.o.}^x$ and $H_{s.o.}^z = 0$ in Eq. (1). Scattering will cause this precession to be randomized, analogous to motional narrowing in electron-spin resonance, leading to a spin-dephasing rate,

$$\tau_{s.o.}^{-1} = \langle \Delta E_c^2 \rangle \tau_{tr} / 4\hbar^2. \quad (3)$$

Here $\langle \Delta E_c^2 \rangle$ is the Fermi-surface-average variance of ΔE_c and $\Delta E_c / 2\hbar$ is the precession frequency. Since $H_{s.o.} \propto (\tau_{s.o.} \tau_{tr})^{-1}$ and $H_{tr} \propto \tau_{tr}^{-2}$, Eq. (3) implies that $H_{s.o.}$ is independent of H_{tr} at a fixed electron density.

TABLE I. Device parameters for GaAs/AlGaAs MOSFETs. Values for N_s and μ are given at $V_G = 0$, $T = 4.2 \text{ K}$.

Device	Spacer thickness (\AA)	N_s (10^{15} m^{-2})	μ ($\text{m}^2/\text{V sec}$)
1016-4a	20	6.4	4.36
1016-5b	20	6.4	7.5
1017-C2a	40	6.1	10.7
G131 ^a	20	5.6	7.28

^aUngated device.

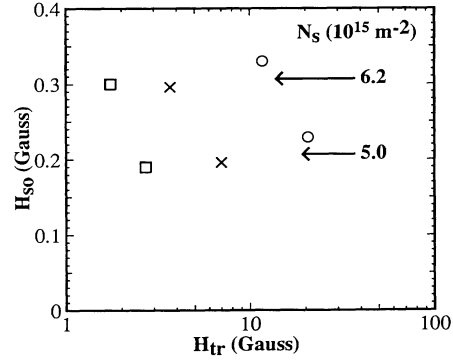


FIG. 2. Spin-orbit field as a function of transport field. At fixed density the variation in H_{tr} is caused by differences in mobility. The squares indicate device 1017-C2a, the crosses indicate 1016-5b, and the circles indicate 1016-4a. The lower set corresponds to $N_s = 5 \times 10^{15} \text{ m}^{-2}$ and the upper set to $N_s = 6.2 \times 10^{15} \text{ m}^{-2}$. Densities are as stated, to within $\pm 2\%$.

Standard GaAs/Al_{0.3}Ga_{0.7}As (100) modulation-doped heterostructures were grown by molecular-beam epitaxy with 20- \AA (wafer 1016) and 40- \AA (wafer 1017) spacer layers, from which 0.1 mm \times 1.6 mm Hall bars were etched. The entire device was covered with an insulating layer of SiO₂ and a Ti-Au (nonmagnetic) gate metal. Details of these devices will be published elsewhere. These wafers and devices allow us to have differing electrostatic confinements and mobilities with the same carrier concentration. The carrier density was inferred from Hall-effect measurements. Because of the small magnetic fields involved, care was taken to remove sources of nonuniformity and magnetic noise. Despite this, we were unable to resolve fields $\lesssim 20 \text{ mG}$, and we attribute this resolution limit to sample nonuniformity.

Table I is a summary of the device parameters. The magnetoconductance measurements were performed at temperatures from 0.4 to 4.2 K.

By fitting the magnetoconductance data with Eq. (1) we deduce $H_{s.o.}$, which we plot in Fig. 2 as a function of H_{tr} for different devices at two fixed densities. Gate voltage is used to set a density for the three devices. H_{tr} is then determined by the relation $H_{tr} = e/4\pi\hbar N_s \mu^2$, where μ is the mobility. Since $H_{s.o.}$ remains nearly constant while H_{tr} varies over an order of magnitude, we conclude that the Elliott mechanism is not the source of spin-orbit scattering in this system. In addition, it is known that the dominant scattering centers in these devices are remote ionized donors, which would produce negligible spin-orbit scattering by the Elliott mechanism. The only scattering mechanism that predicts a spin-orbit rate inversely proportional to the transport rate (i.e., $H_{s.o.}$ independent of H_{tr}) is the DP mechanism. We interpret the data of Fig. 2 as an indication that the DP spin-relaxation mechanism dominates in this range of density and mobility.

The conduction-band splitting results from electronic

interactions with the electric fields. In bulk GaAs, the electric field is the local Ga-As dipole. The energy splitting due to this inversion asymmetry has the form [1]

$$\Delta E_c = 2a_{42}[k^2(k_x^2k_y^2 + k_x^2k_z^2 + k_y^2k_z^2) - 9k_x^2k_y^2k_z^2]^{1/2}. \quad (4)$$

Reducing Eq. (4) to two dimensions involves including the confinement perturbation in the Hamiltonian before considering the conduction-band spin splitting. A simple argument can be made that, because there is a standing wave in the confinement (z axis) direction, there is no moving reference frame which will transform an electric field into a magnetic field. Averaging ΔE_c^2 over the Fermi surface, we find that

$$\langle \Delta E_c^2 \rangle = \frac{1}{2} a_{42}^2 k^6. \quad (5)$$

Using these definitions, the spin-orbit field is

$$H_{s.o.} = \left[\frac{\hbar}{4De} \right] \left[\frac{\langle \Delta E_c^2 \rangle \tau_{tr}}{4\hbar^2} \right] = \left[\frac{m^{*2}}{4\pi\hbar e N_s \tau_{tr}} \right] \left[\frac{\pi^3 a_{42}^2 N_s^3 \tau_{tr}}{\hbar^2} \right] = \eta N_s^2, \quad (6)$$

where N_s is the electron density. For GaAs we calculate $\eta = 7.2 \text{ mG}/(10^{15} \text{ m}^{-2})^2$, using a recent band-structure calculation that has found $a_{42} = 24 \text{ eV}\text{\AA}^3$ [13]. The density dependence of $H_{s.o.}$ is shown in Fig. 3. A least-squares fit by Eq. (6) of the $H_{s.o.}$ data gives an experimental value of $\eta = 8.5 \pm 0.6 \text{ mG}/(10^{15} \text{ m}^{-2})^2$ which compares well with the calculated value given above. Our value of η leads to an experimentally determined value of $a_{42} = 26.1 \pm 0.9 \text{ eV}\text{\AA}^3$ which should be compared to the value $a_{42} = 21 \text{ eV}\text{\AA}^3$ derived from optical measurements [6].

Malcher, Lommer, and Rössler [14] have calculated

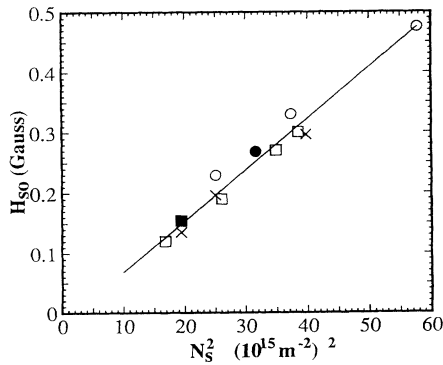


FIG. 3. Spin-orbit field as a function of N_s^2 for all of our devices. Notation is consistent with Fig. 2. In addition the solid circle is datum from device G131 and the solid square is the datum of Kawaji *et al.* The line is a least-squares fit by $H_{s.o.} = a + \eta N_s^2$ with $\eta = 8.5 \pm 0.6 \text{ mG}/(10^{15} \text{ m}^{-2})^2$ and $a = -16 \pm 18 \text{ mG}$.

the zero-field energy splitting in GaAs heterostructures due to the inversion asymmetry and interface spin-orbit (Rashba) terms. In an inversion layer, there is an electric field from the electrostatic confinement leading to the Rashba term, $(a_{46}k\langle E_z \rangle)^2$, where a_{46} is a band-structure parameter and $\langle E_z \rangle$ is the wave-function-average electrostatic field [15]. Lommer and co-workers [14,16] predict that the Rashba term is small in GaAs, but not in narrow-band-gap semiconductors. The inversion asymmetry term divides into two parts. The first part is the same as our Eq. (5) which corresponds to an effective magnetic field perpendicular to the wave vector. The second part, $(2a_{42}k\langle d^2/dz^2 \rangle)^2$, which is calculated to be larger, corresponds to an effective magnetic field parallel to the wave vector.

It is important to note the quadratic dependence of $H_{s.o.}$ on N_s displayed in Fig. 3. A weaker dependence would indicate a spin splitting evolved from something other than the bulk k^6 term in Eq. (5). The k^2 inversion asymmetry term leads to a value of $H_{s.o.}$ independent of N_s . Similarly, the interface electric-field effect would lead to a linear dependence. The only observed dependence is the quadratic term involving the bulk crystal fields. The presence of these additional terms may induce an overestimate of a_{42} which better low-density data would resolve.

At densities lower than $4 \times 10^{15} \text{ m}^{-2}$, we could no longer observe a conductance minimum (see Fig. 1) at our lowest temperature. As density is decreased, both H_{tr} and H_ϕ increase, while $H_{s.o.}$ decreases. If $H_{s.o.} < H_\phi$, the spin-orbit scattering broadens the magnetoconductance without forming a minimum. Sample inhomogeneities also broaden the magnetoconductance. To avoid confusion, we only considered the determination of $H_{s.o.}$ to be reliable when a clear conductance minimum was observed. At high density, we have three major limitations to the determination of $H_{s.o.}$: small signal strength, second subband effects, and applicability of Eq. (1). The conductivity increases with N_s , leading to a smaller measured signal ($\Delta\sigma/\sigma$). Depending on the shape of the depletion layer, the second electric subband begins to populate at $N_s \sim 8 \times 10^{15} \text{ m}^{-2}$, leading to an additional phase-breaking process as well as a parallel conducting path. Finally, the validity of Eq. (1) implies the constraint $0.5H_{tr} \gtrsim 4H_{s.o.}$. If this condition is not met, the conductance minimum is no longer in a range where the present theory applies.

Our results now allow a new interpretation of previous antilocalization experiments on III-V semiconductors. Poole, Pepper, and Hughes [17] measured density-dependent antilocalization in InP metal-oxide-semiconductor field-effect transistors (MOSFETs). Using their data, we find that $H_{s.o.}$ is quadratic in density, giving a value of $\eta = 3.5 \pm 0.3 \text{ mG}/(10^{15} \text{ m}^{-2})^2$. From band parameters [18], a_{42} is estimated, yielding $\eta = 3.9 \text{ mG}/(10^{15} \text{ m}^{-2})^2$ for InP. Kawaguchi [19] has observed antilocalization in InAs with a value of $H_{s.o.} \sim 200 \text{ G}$ at

$N_s = 1.5 \times 10^{16} \text{ m}^{-2}$. Without a density dependence, it is not possible to deduce the relative roles of the crystal field and the Rashba effect in InAs.

The qualitative difference between the k^2 and k^6 terms is the sense of the effective magnetic field with respect to the velocity. The k^6 nature of the splitting has been measured by weak antilocalization in both GaAs and InP. The fact that a k^2 -dependent splitting has not been measured indicates either that this component of the splitting is small or that a weak antilocalization measurement is not sensitive to precession about an axis parallel to the motion of the electron.

In conclusion, weak antilocalization is used to observe spin-orbit scattering in GaAs/AlGaAs MOSFETs. The mobility independence of $H_{s.o.}$ shows that the dominant spin-dephasing mechanism is that of D'yakanov and Perel'. The density dependence indicates that this is caused by the conduction-band spin splitting due to crystal fields. Our results allow an interpretation of antilocalization measurements in III-V semiconductors in terms of band-structure parameters.

We would like to thank C. A. Richter for his experimental help. This work was supported in part by the National Science Foundation under Grants No. DMR 82-13080 and No. ECS-8509135.

^(a)Present address: Institute of Electronic Structure and Laser, Foundation for Research and Technology, Hellas, P.O. Box 1527, Heraklion 711 10, Greece.

[1] G. F. Dresselhaus, *Phys. Rev.* **100**, 580 (1955).

[2] B. Das, S. Datta, and R. Reifenberger, *Phys. Rev. B* **41**, 8278 (1990).

[3] J. Luo, H. Munekata, F. F. Fang, and P. J. Stiles, *Phys.*

Rev. B **41**, 7685 (1990).

[4] D. Stein, K. von Klitzing, and G. Weimann, *Phys. Rev. Lett.* **51**, 130 (1983).

[5] A. H. Clark, R. D. Burnham, D. J. Chadi, and R. M. White, *Phys. Rev. B* **12**, 5758 (1975).

[6] A. G. Aronov, G. E. Pikus, and A. N. Titkov, *Zh. Eksp. Teor. Fiz.* **84**, 1170 (1983) [*Sov. Phys. JETP* **57**, 680 (1983)].

[7] S. Kawaji, K. Kuboki, H. Shigeno, T. Nambu, J. Wakabayashi, J. Yoshino, and H. Sakaki, in *Proceedings of the Seventeenth International Conference on the Physics of Semiconductors, San Francisco, 1984*, edited by J. D. Chadi and W. A. Harrison (Springer-Verlag, New York, 1985), p. 413.

[8] G. Bergmann, *Phys. Rep.* **107**, 1 (1984).

[9] M. I. D'yakanov and V. I. Perel', *Zh. Eksp. Teor. Fiz.* **60**, 1954 (1971) [*Sov. Phys. JETP* **33**, 1053 (1971)].

[10] S. Hikami, A. I. Larkin, and Y. Nagaoka, *Prog. Theor. Phys.* **63**, 707 (1980).

[11] R. J. Elliott, *Phys. Rev.* **96**, 266 (1954).

[12] B. L. Altshuler, A. G. Aronov, D. E. Khmel'nitskii, and A. I. Larkin, in *Quantum Theory of Solids*, edited by I. M. Lifshits (Mir, Moscow, 1982).

[13] P. Pfeffer and W. Zawadzki, *Phys. Rev. B* **41**, 1561 (1990).

[14] F. Malcher, G. Lommer, and U. Rössler, *Superlattices Microstruct.* **2**, 267 (1986).

[15] Y. A. Bychkov and E. I. Rashba, *J. Phys. C* **17**, 6039 (1984).

[16] G. Lommer, F. Malcher, and U. Rössler, *Phys. Rev. Lett.* **60**, 728 (1988).

[17] D. A. Poole, M. Pepper, and A. Hughes, *J. Phys. C* **15**, L1137 (1982).

[18] I. M. Tsidil'kovski, *Band Structure of Semiconductors* (Pergamon, New York, 1982).

[19] Y. Kawaguchi, I. Takayanagi, and S. Kawaji, *J. Phys. Soc. Jpn.* **56**, 1293 (1987).